Experimental Observations of the Expansion of an Optical-Field-Induced Ionization Channel in a Gas Jet Target

M. Dunne, T. Afshar-Rad, J. Edwards, A. J. MacKinnon, S. M. Viana, and O. Willi
Blackett Laboratory, Imperial College of Science, Technology and Medicine, London SW7 2BZ, United Kingdom

G. Pert
Department of Physics, University of York, York, United Kingdom
(Received 25 January 1993; revised manuscript received 12 October 1993)

The evolution of an optical-field-ionized channel created by a 3.5 ps KrF laser pulse in a low density nitrogen gas jet target (10^{17} ions cm^{-3}) has been studied using Moiré deflectometry. This allowed the density profiles in the channel and its lateral expansion to be quantitatively measured for the first time. The results were reproduced well by hydrocode simulations and analytical models. In addition, structured Raman backscatter signals indicated very low longitudinal electron velocities in the rising part of the pulse, as confirmed by 2D particle-in-cell code simulations.

PACS numbers: 52.50.Jm, 32.80.Rm, 52.35.Tc

The properties of highly ionized laser-induced cylindrical plasmas in gaseous targets have been the subject of much theoretical discussion [1–5] and, more recently, experimental investigation [6–11]. Plasmas produced by optical-field-induced (OFI) ionization are inherently different from those in which collisional processes are dominant. Plasmas can be created in which the ionization stage achieved may be far in excess of that which would be attained if thermal collisions alone governed the ionization. Information on the spatial and temporal evolution of the electron density profile of these OFI ionized plasmas is invaluable for many applications, as detailed in [1]. The behavior of these transient channels has a more fundamental interest in the study of nonequilibrium high temperature explosions. Very few clean experimental data exist on such explosions, with previous measurements having used shock tubes or back filled laser-irradiated chambers and pulse lengths longer than characteristic hydrodynamic time scales [12]. In addition, the possibility of producing a cold (< 100 eV), highly ionized, low density plasma channel has led to the suggestion of a number of recombination extreme ultraviolet (XUV) laser schemes. These offer the distinct advantage of being able to significantly reduce the average electron energy after the turnoff of the pumping pulse, so enabling the required rapid recombination to take place. Furthermore, x-ray lasers in optical-field-ionized plasmas require very low driver energy and can allow lasing to the ground state [2]. Consequently, experimental verification of the production of such plasmas is of central importance to short pulse x-ray laser production. Even the process of OFI ionization may, however, prove to be insufficient to reduce the residual electron temperature to the level required for high efficiency, as has been discussed [3,4]. In this situation the role of the lateral expansion of the plasma column becomes critical since this will determine the rate of cooling of the ionized channel.

This Letter presents experimental measurements on the evolution of an optically ionized channel by a high intensity, short wavelength picosecond laser pulse using Moiré deflectometry. In addition, structure in stimulated Raman backscatter spectra was observed from a number of discrete ionization stages. For the first time the crucial issue of how a cylindrical plasma channel expands after a heating pulse, whose length is short in comparison with the hydrodynamic response time, is addressed. A 1D cylindrical geometry hydrocode accurately reproduced the expansion characteristics of the channel. Analytical models matched the asymptotic behavior of the expansion and established levels of heating consistent with the hydro and particle-in-cell (PIC) code predictions through inverse bremsstrahlung absorption.

The experiments were performed on the SPRITE KrF gas laser at the Rutherford Appleton Laboratory using a 3.5 ps, 248 nm, 1.5 J, linearly polarized pulse. The beam was focused by an $f/5$ off-axis paraboloid mirror to a focal spot size of approximately 30 μm, achieving intensities on target of around 2×10^{16} W cm^{-2}. The use of an ultraviolet (UV) laser and a relatively large focal spot allowed refractive and ponderomotive force effects to remain insignificant [13]. A small fraction of the beam was split off in order to provide a temporally independent probe beam, perpendicular to the heating beam, for the Moiré deflectometry system, which supplied snapshot information on the electron density gradients and absolute electron densities for discrete times up to 1 ns after the heating pulse. The magnification of the system was 100× with a spatial resolution of 1 μm at the target plane. The timing of the probe beam relative to the heating beam was accurate to 3 ps. The target consisted of a pulsed supersonic gas jet which delivered nitrogen through a simple DeLaval nozzle. This jet formed a cylindrical gas column perpendicular to the axis of laser irradiation with a diameter of around 1 mm, yielding a particle density of $(1.25\pm0.25)\times10^{17}$ atoms cm^{-3} at the point of interaction. At these densities electron recombination rates are negligible, allowing the difficult problem of modeling recombination in an evolving plasma to be ignored. The

0031-9007/94/72(7)/1024(4)$06.00

light backscattered during the heating pulse was monitored with a 1200 l/mm grating spectrometer with 2.5 Å resolution. In addition, a time integrating XUV (10 to 40 Å) toroidal grating spectrometer recorded the K-shell emission from the channel, supplying information on the peak ionization stage.

Moiré probe measurements taken during and immediately after the heating pulse (at $\Delta t = 0$ and 5 ps) and time-integrated stimulated Raman backscatter (B-SRS) signals provided information on the initial laser created plasma channel. This channel was formed through optical ionization processes which have been extensively studied elsewhere (see, for example, [3,6]) in which the characteristic Keldysh parameter was of the order of unity. By employing a simple Coulomb-barrier model [3] the threshold intensity required to reach each of the different ionization stages can be calculated; it was found that intensities of 2.3×10^{15}, 9×10^{15}, 1.4×10^{16}, and 1×10^{19} W cm^{-2} were required for the Be-, Li-, He-, and H-like stages, respectively. Collisional ionization can be neglected at these low densities. The plasma therefore reaches a He-like peak ionization stage, as confirmed by the toroidal grating XUV spectrometer, with a substantial fraction still existing as Li-like ions since the He-like intensity threshold was only just achieved. On less intense shots (1×10^{16} W cm^{-2}) the presence of He-like emission was not observed, confirming the simple intensity threshold estimate.

Figure 1(a) shows a Moiré deflectogram taken immediately after the heating pulse ($\Delta t = 5$ ps), in which the fringe shifts are directly proportional to the local spatial density gradients. Only the central section (approximately 120 μm in length) of the laser focus is shown for clarity. A strong discontinuity can be observed in the fringe pattern, indicating the radial extent of the ionizing laser profile. The Abel-inverted absolute densities for this time are shown in Fig. 1(b). An important feature to note is the axial stability of the channel, showing no evidence of any self-focusing or radial oscillations. Such stability is important if the channel is to be used as a waveguide for secondary pulses [1].

The backscattered light was redshifted relative to the fundamental and was split into three separate spectral features, with the long wavelength spike shifted by approximately 15 Å (see Fig. 2). These features correspond to weakly coupled B-SRS from three different ionization stages present in the plasma, with the strong, central spectral feature corresponding to the dominant Li-like stage. Note that stimulated Brillouin scattering or Compton scattering effects cannot explain the observed features. For the dominant plasma conditions the growth rate for B-SRS from a finite pump [5,9] is calculated to be of the order of 150 fs, significantly shorter than the 3.5 ps heating pulse length. The three discrete optically ionized stages are produced either at different times in the laser-gas interaction, or in different spatial regions of the target as a result of the falloff of the laser profile. The discrete nature of the features results from the rapidity of the optical ionization, which occurs on time scales far shorter than the B-SRS growth times. On the less intense shots (1×10^{16} W cm^{-2}) the longest wavelength spike was not observed since the laser intensity was not sufficient to ionize the plasma to a He-like state.

The observed B-SRS shifts are in good agreement with the electron densities measured during the pulse [8]. This indicates that the thermal contribution to the dispersion relation, which is important at these low densities, must be small. More specifically, the longitudinal velocities of the ionized electrons must remain low for a number of SRS growth times after ionization. This scattering must occur close to the peak of the pulse for electrons producing the He-like feature. By using the peak electron density known from the Moiré data taken during the heating pulse, the plasma frequency for each ionization stage can be determined, allowing the thermal contribution to the Raman shift to be calculated using phase-matching conditions and the Bohm-Gross dispersion equation [9]. For each of the discrete electron densities corresponding to the three optically ionized stages, the calculated longitudinal velocities were consistent with temperatures of less than 1 eV. An increase in temperature to only 5 eV would result in a wavelength shift of 31 Å, contrary to the observations. The small uncertainties in the calculation of the peak electron density do not alter the 1 eV temperature constraint.

The degree of plasma heating has been estimated from

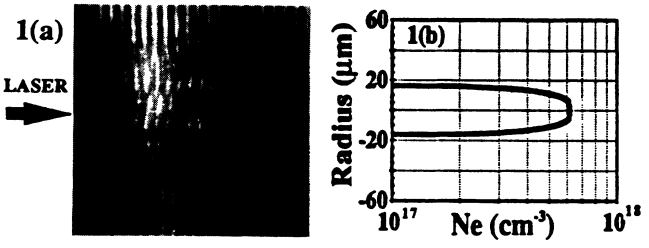

FIG. 1. (a) Moiré deflectometer fringe pattern at the end of the heating pulse ($\Delta t = 5$ ps). (b) The Abel-inverted density profile for this shot [on the same spatial scale as (a)]. The density profile obtained is accurate to within $\pm$ 10% and is primarily limited by uncertainties in the fringe shift measurements.

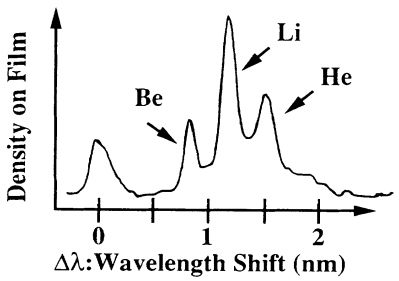

FIG. 2. Densitometer lineout of the time-integrated, spectrally resolved backscattered light.

a 1D propagation-ionization model [4]. It was found that above-threshold ionization heating contributed less than 5 eV to the final plasma temperature in these simulations, whereas inverse bremsstrahlung (IB) was predicted to heat the gas to up to 35 eV [14] once the 50% reduction due to the Langdon effect was taken into account. This level of IB heating was also confirmed by a simple analytical estimate of the absorption which distributed the one-way energy absorption fraction throughout an optically ionized electron distribution, predicting a temperature of 34 eV. Details of this model will be published elsewhere. The low density of the plasma results in an electron-ion collision frequency for the quivering electrons of approximately 7.1×10^{9} sec^{-1}. Consequently, only very few electrons (around 1 in 40) will undergo energy absorbing collisions during the laser pulse, with this IB heating occurring predominantly after the optical ionization has taken place. A nonthermal electron distribution will thus be created, with a Maxwellian forming only on time scales of the order of the electron-electron collision time (a few ps). This leads to a qualitative understanding of the B-SRS results. For a more quantitative analysis of the temperature evolution in the initial plasma, 2D PIC code simulations were performed [15]. IB absorption was represented through the use of a Monte Carlo scattering term [3]. The calculated evolution of the heating in the ionizing channel is shown in Fig. 3, where an average energy of 3.5 eV is predicted in the longitudinal dimension at the time when He-like ions are produced (0.65 ps), in reasonable agreement with the Raman observations. In addition to detailing the energy distribution during the rising edge of the pulse, the 2D PIC code provided an estimate of the subsequent heating mechanisms in the channel. IB absorption was seen to dominate, being most effective later in the pulse, producing a final energy content of 27 eV. B-SRS is expected to be heavily Landau damped in the latter part of the pulse, when the longitudinal electron temperature rises above a few eV. The pulse shape used in the calculations was one thought to best represent the actual experimental pulse.

The temporal evolution of the hot, central channel was studied with the Moiré deflectometer by delaying the probe beam with respect to the heating beam. A rapid expansion of the laser-created channel was observed, in which the strong discontinuity seen in Fig. 1 propagated into the ambient gas with an initial velocity of $(4.4\pm0.6)\times10^{6}$ cm/s. Because of the extremely low rate of electron recombination at this low gas density (radiative recombination from He-like to Li-like ions occurs on time scales of many tens of nanoseconds for a nitrogen plasma at a few tens of eV), the central plasma channel effectively remains at the ionization stage at which it was created, with low levels of collisional ionization occurring at the position of the propagating shock front. The electron density evolution in the center of the channel consequently follows the dependence of the ion density evolution. The degree of ionization induced by the propagating front will typically be of the order of or less than 1, resulting in electron densities outside of the original laser focal region less than or equal to the local ion density. The rate of expansion was observed to reach an asymptotic limit (going as $t^{1/2}$) within 1 ns of the heating pulse, with the expansion characteristics after 500 ps being accurately modeled by a cylindrical geometry, strong shock explosion model adapted from [16].

The expansion was also modeled using a 1D Lagrangian hydrocode, MEDUSA [17], in cylindrical geometry and with a modified absorption routine which deposited a stated fraction of the incident energy on axis in a channel of 30 μm diameter. Both the spatial and temporal profiles of the laser were taken to be Gaussian, with the spatial profile cut off at the $1/e$ point. The ions were modeled by an ideal gas equation of state (EOS) and the electrons by a Thomas-Fermi–type EOS, streaming radially outwards according to a flux-limited ($f=0.1$) Spitzer

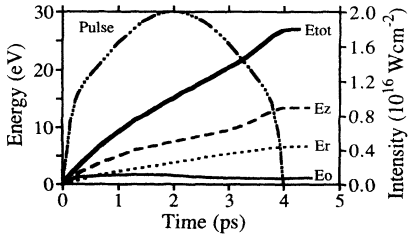

FIG. 3. 2D PIC simulations of the heating of the optically ionized channel. The evolution of the energy in the longitudinal (E_z) and radial (E_r) dimensions is shown, along with the combined energy (E_{tot}). Also shown is the evolution if collisional heating is ignored (E_0). The laser pulse shape used is also shown.

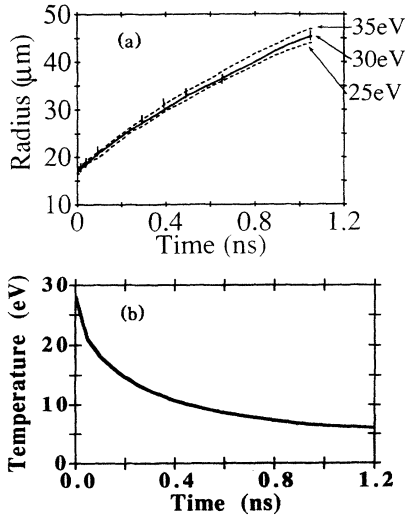

FIG. 4. (a) Simulations of the expansion of the plasma channel compared with experimental data points (vertical bars). The best fit to the data (solid line) was for an initial electron temperature of 30 eV, (b) predicted temperature evolution in the center of the channel for the 30 eV simulation.

heat flow model. The EOS self-consistently accounted for the energy required to ionize the plasma. The hydrocode did not attempt to realistically model the laser absorption, the optical ionization, or any plasma heating processes other than collisional and shock heating. Ionization in the hydrocode used a steady-state model and was consequently post processed using a time-dependent, non-LTE, screened-hydrogenic, average-ion ionization code similar to XSN [18]. This was necessary in order to model the transient ionization occurring at the expanding wave front, where extremely low collisional ionization rates produced a plasma far removed from the steady state.

The radius of the channel at 1 ns was taken to act as a fixed point in the hydrocode simulations as the expansion had attained its asymptotic nature by this time. The fraction of absorbed energy acted as a free parameter and was altered until the radius of the simulated channel at 1 ns after the heating pulse matched the observed radius. This is equivalent to varying the initial temperature of the cylindrical explosion. The radial extent of the simulated expansion was then compared with the observations for times earlier than the 1 ns fixed point, resulting in good agreement as shown in Fig. 4(a). A noticeably different expansion profile is obtained with a change in energy absorption sufficient to produce a 5 eV change in the initial plasma temperature. The best fit to the data was obtained with a temperature of 30 ± 5 eV. This is in good agreement with the independent PIC code predictions, confirming that the rate of expansion provides an accurate indication of the energy content in the channel at the end of the heating pulse.

The rapid, expansion-induced cooling of the central channel was determined from the hydrocode simulations [see Fig. 4(b)], with the temperature predicted to drop from 30 to 15 eV in 200 ps. In addition, by comparing the positions of the ion and electron density fronts at each time step in the simulation, the initial expansion was found to be driven by an electron conduction wave up to 200 ps after the pulse and that subsequent evolution was governed by the ion shock wave, with the density falling from 6.2×10^{17} to 5.6×10^{17} e^-/cm^3 in the first 500 ps. Flux limited heat flow was required in the simulations in order to reproduce the steep shock front observed in the experiment. In contrast, free-streaming conduction acted to significantly broaden the shock front and also reduced the energy required in the initial plasma to drive the expansion. Even with the reduction in initial energy, these simulations could not reproduce the observed channel evolution, particularly during the initial ($t < 200$ ps) thermal conduction period of the expansion.

Because of the steep nature of the shock front, the temperature scale lengths in the region of the front were often comparable to the mean free paths of even the mean velocity electrons (of the order of 1 μm). Such a situation can lead to severe nonlocal heat flow effects [19], which were probably responsible for a weakly ionizing precursor observed to penetrate 10 to 20 μm into the neutral gas ahead of the main front.

In summary, the temporal evolution of an optical-field-induced ionization channel has been observed and the global features of the expansion accurately reproduced by a 1D cylindrical-geometry hydrocode. The initial expansion of the channel was dominated by electron thermal conduction, with subsequent evolution governed by the propagation of the strong ion shock wave. Structure in Raman backscatter spectra was observed and used to infer low longitudinal electron velocities in the initial channel, as confirmed by 2D PIC code simulations.

The authors would like to thank S. C. Rae and K. Burnett for providing valuable computational results. We also thank R. A. Smith and J. Tisch for the construction of the gas jet driver. We are indebted to the SPRITE laser and target area staff of the Central Laser Facility for their support throughout the experiment. This work was funded by the SERC.

[1] P. Sprangle and E. Esarey, Phys. Fluids B **4**, 2241 (1992).
[2] J. Peyraud and N. Peyraud, J. Appl. Phys. **43**, 2993 (1972).
[3] B. M. Penetrante and J. N. Bardsley, Phys. Rev. A **43**, 3100 (1991).
[4] S. C. Rae and K. Burnett, Phys. Rev. A **46**, 2077 (1992).
[5] D. C. Eder, P. Amendt, and S. C. Wilks, Phys. Rev. A **45**, 6761 (1992).
[6] S. Augst *et al.*, Phys. Rev. Lett. **63**, 2212 (1989).
[7] W. P. Leemans *et al.*, Phys. Rev. Lett. **68**, 321 (1992).
[8] M. D. Perry *et al.*, Opt. Lett. **17**, 523 (1992).
[9] C. B. Darrow *et al.*, Phys. Rev. Lett. **69**, 442 (1992).
[10] T. Auguste *et al.*, Opt. Commun. **89**, 145 (1992).
[11] A. L'Huillier, K. J. Schafer, and K. C. Kulander, Phys. Rev. Lett. **66**, 2200 (1991).
[12] J. C. Griesemann and M. Decroisette, J. Appl. Phys. **50**, 3915 (1979).
[13] P. A. Amendt *et al.*, Proc. SPIE Int. Soc. Opt. Eng. **1860**, 140 (1993).
[14] S. C. Rae (private communication).
[15] G. Pert, Annual Report to the Central Laser Facility, No. RAL-93-031, 82-83, 1993 (unpublished).
[16] Ya. B. Zel'dovich, and Yu. P. Raizer, *Physics of Shock Waves and High Temperature Hydrodynamic Phenomena* (Academic, New York, 1966).
[17] J. P. Christiansen, D. E. T. F. Ashby, and K. V. Roberts, Comput. Phys. Commun. **7**, 271 (1974).
[18] W. A. Lokke and W. H. Grasberger, LLNL Report No. UCRL-52276, 1977 (unpublished).
[19] A. R. Bell, R. G. Evans, and D. J. Nicholas, Phys. Rev. Lett. **46**, 243 (1981).

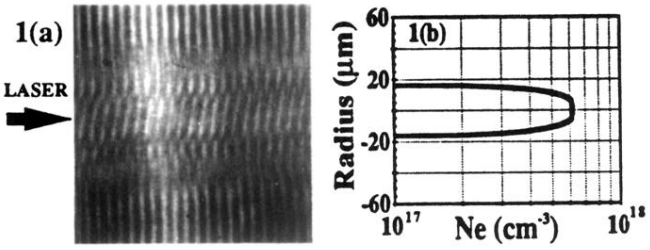

FIG. 1. (a) Moiré deflectometer fringe pattern at the end of the heating pulse ($\Delta t = 5$ ps). (b) The Abel-inverted density profile for this shot [on the same spatial scale as (a)]. The density profile obtained is accurate to within $\pm 10\%$ and is primarily limited by uncertainties in the fringe shift measurements.